Small-Grid Dithers for the JWST Coronagraphs

Charles-Philippe Lajoie*[a], Rémi Soummer[a], Laurent Pueyo[a], Dean. C. Hines[a], Edmund P. Nelan[a], Marshall Perrin[a], Mark Clampin[b], John C. Isaacs[a], and The JWST Coronagraphs Working Group.

[a]Space Telescope Science Institute, 3700 San Martin Drive, Baltimore, MD, USA 21210;
[b]NASA Goddard Space Flight Center, 8800 Greenbelt Rd, Greenbelt, MD 20771

ABSTRACT

We discuss new results of coronagraphic simulations demonstrating a novel mode for JWST that utilizes sub-pixel dithered reference images, called Small-Grid Dithers, to optimize coronagraphic PSF subtraction. These sub-pixel dithers are executed with the Fine Steering Mirror under fine guidance, are accurate to ~2-3 milliarcseconds (1-σ/axis), and provide ample speckle diversity to reconstruct an optimized synthetic reference PSF using LOCI or KLIP. We also discuss the performance gains of Small-Grid Dithers compared to the standard undithered scenario, and show potential contrast gain factors for the NIRCam and MIRI coronagraphs ranging from 2 to more than 10, respectively.

Keywords: JWST, coronagraphy, post-processing, exoplanets, circumstellar disks.

1. INTRODUCTION

The James Webb Space Telescope (JWST) will be equipped with a suite of coronagraphic instruments designed to obtain high-contrast imaging of objects such as exoplanets, circumstellar disks, and active galactic nuclei. Together, the Near-Infrared Camera (NIRCam)[1] and the Mid-Infrared Instrument (MIRI)[2] will provide both Lyot and Four-Quadrant Phase Mask (4QPM) coronagraphs and will cover wavelengths ranging from 2 to 23 μm. The standard coronagraphic observation scenario for JWST will provide imaging of a target star (at possibly two roll angles) as well as imaging of a reference star for point-spread function (PSF) subtraction. In general, PSF subtraction is optimal when the reference and target stars are positioned exactly at the same location behind the coronagraphic mask. Despite an expected pointing of 5 milliarcseconds (mas, 1-σ/axis) for small-angle maneuvers (SAM), JWST coronagraphic performance will remain a challenging endeavor and will ultimately be limited by its ability to accurately, and repeatedly, position the target star behind the coronagraphic mask, in particular for MIRI's 4QPM[3].

Advances in post-processing[4,5] in the last decade have pushed the limits of high-contrast imaging by relying on multiple reference stars in order to maximize PSF subtraction. In order to mitigate the sensitivity to position offsets of the JWST coronagraphs and improve the performance of PSF subtraction, flight software changes were implemented. Indeed, recent enhancements to JWST's attitude control system (ACS) now allow for accurate sub-pixel offsets to be performed with the Fine Steering Mirror (FSM) while remaining under Fine Guidance control. These FSM offsets are accurate (~1-2 mas, 1-σ/axis) and efficient, requiring no additional target acquisition and taking only a few seconds to execute compared to over 20 seconds required by the standard SAM. In order to remain in Fine Guidance control, the range of motion supported by these small dithers is restricted to ~1 FGS pixel, or ~69 mas. Small-Grid Dithers (SGDs) is a new strategy that employs these sub-pixel dithers for further improving contrast in coronagraphic observations. SGDs rely on obtaining multiple images of the same reference star separated by small, sub-pixel offsets in order to sample PSF variations across the coronagraph mask and optimize the PSF subtraction using KLIP[4] or LOCI[5].

This communication is a follow-up on our initial results[6]. Here, we present updated results, based on numerical simulations, for both NIRCam and MIRI coronagraphs. In section 2, we discuss the details of operation and implementation of SGDs, and present our main results along with some simulated images in section 3.

*lajoie@stsci.edu; phone +1 410 338-5007

Space Telescopes and Instrumentation 2016: Optical, Infrared, and Millimeter Wave, edited by Howard A. MacEwen, Giovanni G. Fazio, Makenzie Lystrup, Proc. of SPIE Vol. 9904, 99045K · © 2016 SPIE · CCC code: 0277-786X/16/$18 · doi: 10.1117/12.2233032

2. SMALL-GRID DITHERS SIMULATIONS

2.1 Concept & Operational Design

The Small-Grid Dither (SGD) approach is rather simple: observe both the target and reference stars behind the coronagraphic mask using standard coronagraphic acquisition, then dither the reference star behind the mask by 5 to 30 mas along a square grid pattern using the FSM. An example of such a grid is shown in Figure 1 (*left*). The sub-pixel dithers are performed under closed-loop guiding and therefore require no additional target acquisition, although the actual exposure time is increased by a factor approximately equal to the number of dithered observations (assuming the same exposure parameters for the reference star). The performance enhancement of SGDs therefore comes at a non-negligible cost and would only be required for the most challenging science targets that cannot be observed using the standard coronagraphic observing sequence. General observers will be offered SGDs as an option and a careful analysis and justification of the costs and benefits of the approach will be necessary before pursuing it.

SGDs provide a small library of reference images that effectively samples PSF diversity close to the center of the coronagraphic mask. Post-processing optimization algorithms (e.g. LOCI or KLIP) can be used with this small library of PSFs to reconstruct an optimal synthetic reference to be subtracted from the target star image. As part of the coronagraphic data pipeline, the JWST Coronagraphs Working Group is currently considering: (1) implementing various optimization algorithms for effectively processing SGD data; and (2) augmenting the SGD contemporaneous library with additional PSFs from a public library of reference PSFs. Such improvements to the coronagraphic data pipeline will handle the optimization process involved with the new SGD approach and will provide users with optimal, science-ready products.

2.2 Computational Method

Our simulations model the operational scenario described above and use the expected slew accuracy of the observatory as well as the FSM accuracy (~5 mas and ~2 mas at 1-σ/axis, respectively) for determining the position of the target and reference star behind the mask. This target acquisition is assumed to be a random Gaussian process in our simulations. Because of slew uncertainties, the target and reference stars do not end up at the same position behind the mask in most of our simulated grids. These are the cases where using SGD is most beneficial, as shown below. However, in a few of our simulated cases, the target and reference stars do in fact land within 1-2 mas of each other, and in these cases we can expect Classical Subtraction (i.e. 1-to-1 subtraction) to perform quite well.

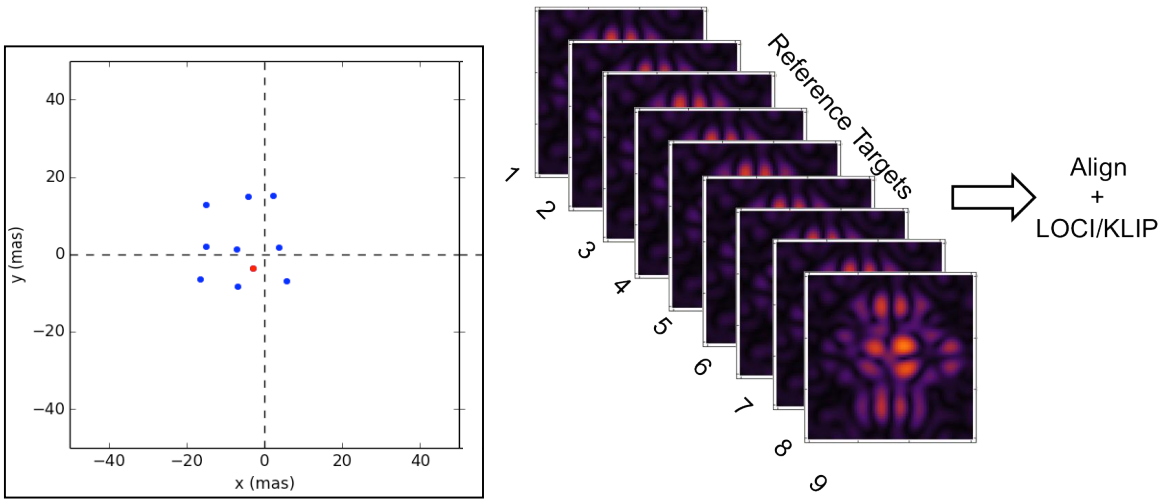

Figure 1. *Left*: Example of Small-Grid Dithers, where the mask is centered on the plot (intersection of dashed line). Given the slew and FSM accuracies, the target star lands on the red dot whereas the reference star is positioned on the grid of blue dots. *Right*: The various reference star images collected are then gathered and individually aligned with the target star, which are then processed using LOCI/KLIP to produce a synthetic PSF that optimizes the PSF subtraction. Multiple random realizations of such target acquisition were simulated in this study.

We use WebbPSF[7] to generate a coronagraphic PSF at each randomly drawn grid position, providing us with a small library of contemporaneous coronagraphic PSFs, similar to in-flight operations, to be used for optimizing the PSF subtraction (Figure 1, *right*). We use WebbPSF's OPD (optical path difference) maps at 136 nm rms and 204 nm rms for NIRCam and MIRI, respectively. For completeness, we also add noise sources such as jitter (7 mas, 1-σ/axis), detector noise, and photon and background noise to our simulated images. We typically generate between 10 and 50 different realizations of SGDs using NIRCam's round and bar occulters and MIRI's 4QPM coronagraphs. The images from each realization of SGDs are then aligned with the target using a simple bi-cubic algorithm, although recent work suggests that Fourier-based alignment algorithms perform better and can further improve the PSF subtraction (L. Pueyo, *priv. comm.*). The library of reference PSFs is then used with LOCI or KLIP to construct a synthetic PSF that matches as closely as possible the target star PSF, which is then subtracted from the latter. Finally, contrast is simply calculated by normalizing the subtracted images by a non-occulted (i.e. no focal plane mask but Lyot stop included) and calculating the azimuthal standard deviation. We are now in the process of improving and standardizing our contrast calculations to use STScI's Exposure Time Calculator covariance matrix approach, which will rely on the multiple realizations of the SGDs we have generated. A summary of all the simulated modes and wavelengths investigated in this work can be found in Table 1.

Table 1 Summary of the simulated coronagraphic modes investigated.

INSTRUMENT	FILTER	FOCAL PLANE MASK
NIRCam	F210M	MASK 210R
NIRCam	F210M	MASK SWB
NIRCam	F430M	MASK 430R
NIRCam	F460M	MASK LWB
MIRI	F1065C	4QPM 1065
MIRI	F1140C	4QPM 1140
MIRI	F1550C	4QPM 1550

3. SIMULATED CONTRAST GAIN

For each SGDs contrast image that we generate, we also process the target star image with a single reference star, which we refer to as Classical Subtraction, in order to directly compare the performance of both methods. Our results are therefore reported in terms of relative performance gains only for now. Absolute contrast curves will be reported in the future. Figures 2, 3, and 4 show the relative gain of SGDs over Classical subtraction for a subset of all the modes investigated, namely MIRI 10.65 μm, NIRCam 2.10 μm (round occulter), and NIRCam 4.60 μm (bar occulter) respectively.

In general, we find that SGDs improve contrast at the coronagraphs' inner working angle by a factor of 3-5 for NIRCam and more than 10 for MIRI. At larger separations, the gain subsides to a factor of 1.5 for NIRCam and between 5 and 10 for MIRI. As expected, MIRI 4QPM coronagraphs benefit the most from SGDs as they are more sensitive to position offsets than the NIRCam Lyot-type coronagraphs.

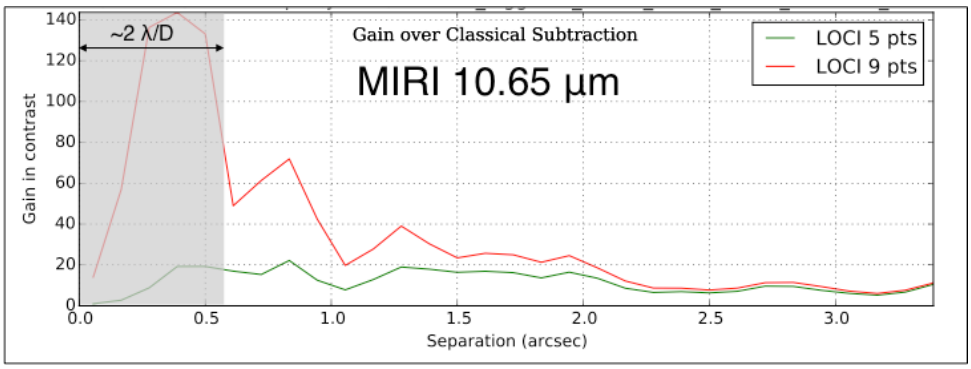

Figure 2. Relative gain in contrast of SGDs compared to Classical Subtraction. Red and green lines are for 9- and 5-point SGD grids, respectively. The gray box is approximately the size of the actual focal plane mask.

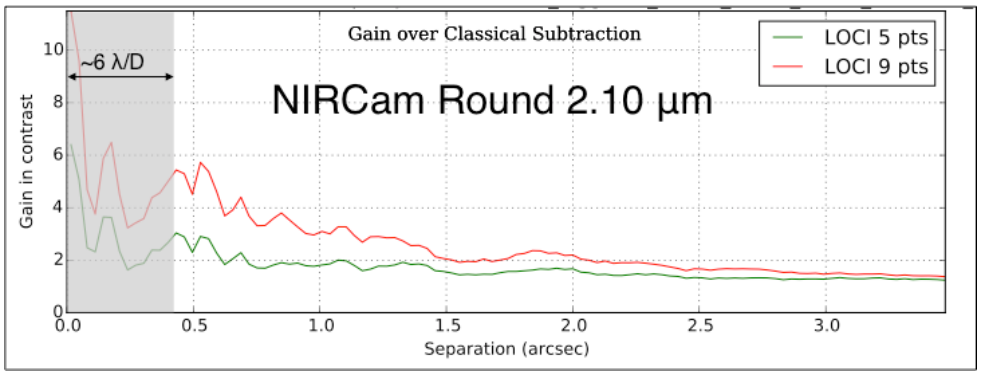

Figure 3. Same as Figure 2 but for NIRCam Round occulter at 2.10 µm.

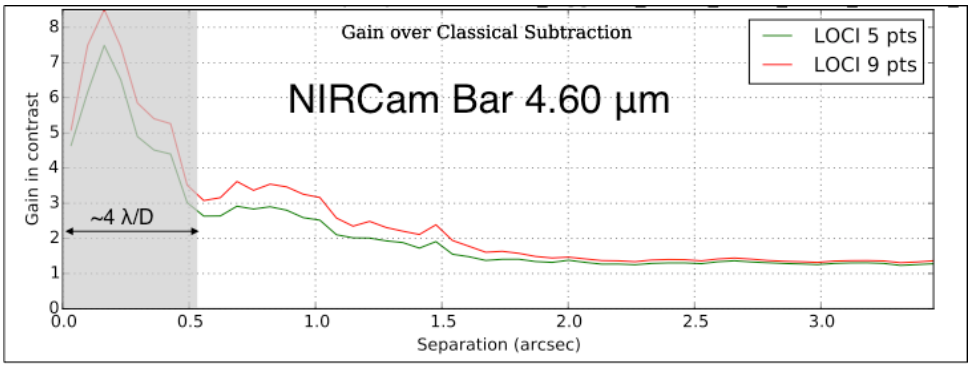

Figure 4. Same as Figure 2 but for NIRCam Bar occulter at 4.60 µm.

As discussed in our initial communication[6], our simulations suggest an optimal grid step size of about 10-20 mas. However, in some cases, we find that the reference star falls far enough from the target star behind the mask that a 10-mas grid step does not encompass the target star. Here, we use 20-mas grid steps in order to ensure that the grid encompasses the target star position behind the mask. Moreover, our simulations suggest that 9-point grids is a good performance compromise, as illustrated in Figure 5, although increasing the number of dithered references could further improve the achievable contrast. Indeed, a gain in contrast of a factor of less than <50% might not be justified by a total exposure time 5 times longer. Based on our results, we therefore

recommend using 9-point square grids, although it remains to be investigated whether NIRCam's bar occulters would benefit from using grids of different shapes (e.g. elongated in one direction or another).

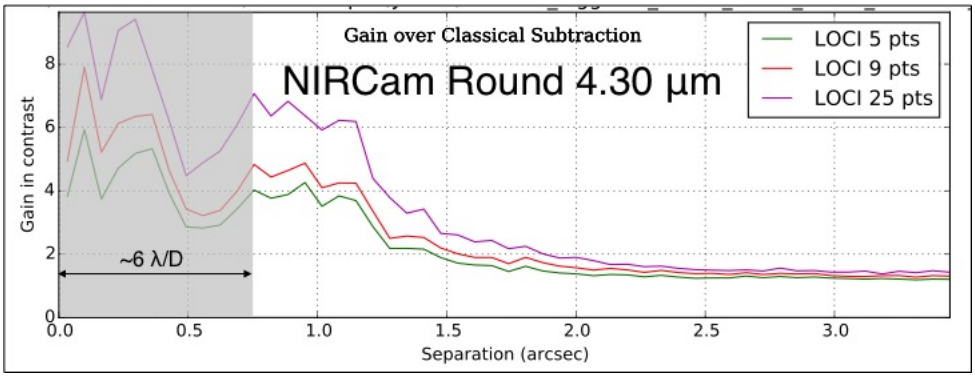

Figure 5. Relative gain of SGD compared to Classical Subtraction for NIRCam's round occulter at 4.30 µm using 5-, 9-, and 25-point grids. Using more grid points improves the contrast at the innermost separations, although the cost of obtaining many more reference images can become prohibitive.

4. SIMULATED IMAGES

We also present simulated images for both NIRCam and MIRI to give the reader a visual appreciation of the relative performance of SGDs compared to Classical Subtraction. We model the case of HR 8799 and use separation and magnitude values published in the literature[8, 9] for the different wavelength bands used here.

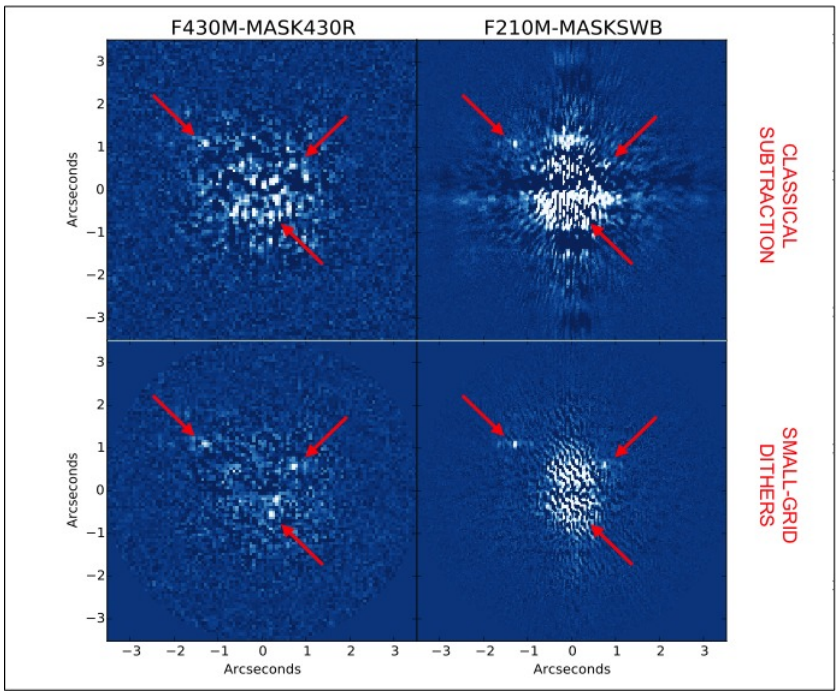

Figure 6. . Simulated images of HR 8799 with NIRCam showing the relative performance of SGDs (*bottom row*) and Classical Subtraction (*top row*) for two different coronagraph modes. The target and reference images are simulated with the same WFE, and the decreased performance of Classical Subtraction is due the relative offset of the reference star behind the mask.

Figures 6, and 7 show randomly selected cases of SGDs and Classical Subtraction for NIRCam and MIRI respectively. The relative performance of SGDs is obvious for both instruments, especially at small separations where SGDs are particularly efficient at removing speckles that Classical Subtraction does not remove.

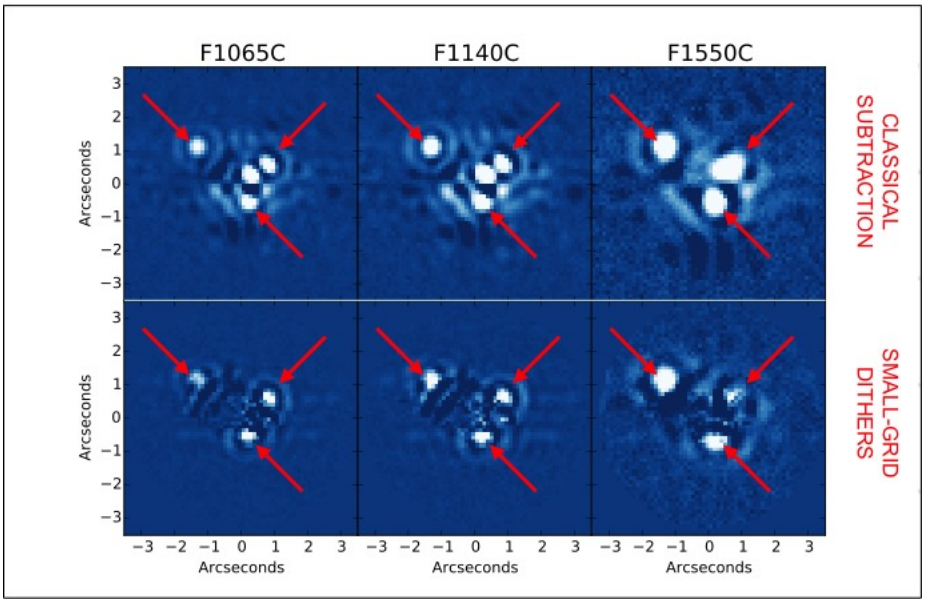

Figure 7. Same as Figure 6 but for the MIRI 4QPM, showing one randomly selected case of target acquisition.

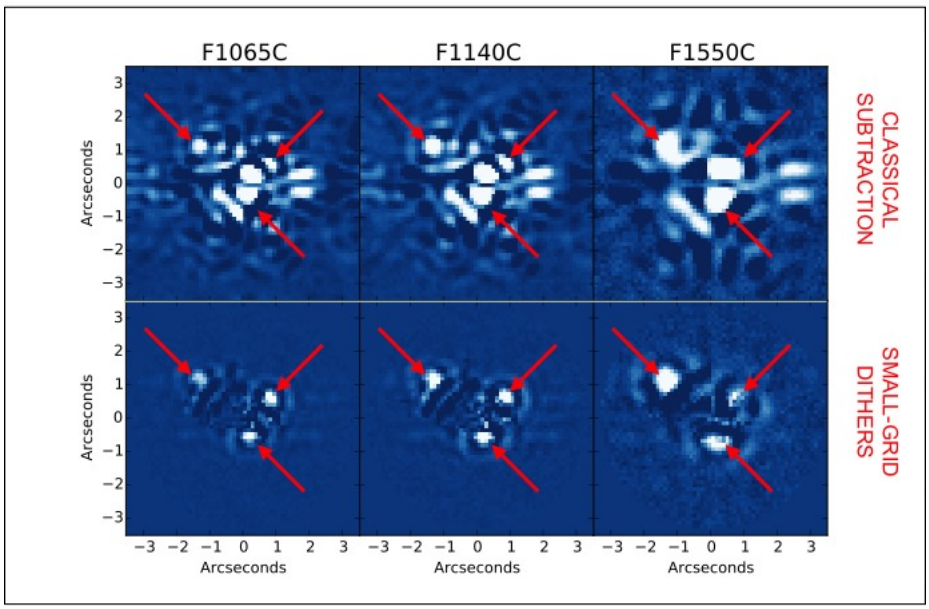

Figure 8. Same as Figure 7 but for a case where the target acquisition match between the target and reference stars does not match as well and the Classical Subtraction performs poorly, showing that SGDs perform robustly and independently of target acquisition.

Figure 8 shows MIRI 4QPM simulated images where the target acquisition for the target and the reference stars did not match as well, and the contrast gain of SGDs is striking. Classical subtraction is much more

sensitive to the accuracy of target acquisition and is somewhat random, whereas SGDs perform robustly and independently of the actual accuracy of target acquisition.

5. CONCLUSIONS

Recent advances in post-processing have pushed the limits of high-contrast imaging to increasingly deeper contrast. Here, we update the results on a new approach that mitigates target acquisition uncertainties and allows for significant performance improvements with only negligible additional overheads. Most importantly, Small-Grid Dithers can be performed while remaining in closed-loop fine guidance, and require no additional target acquisition. Small-Grid Dithers provide a library of contemporaneous reference PSFs that samples the variations in the PSF shape, mitigating the pointing and reproducibility errors and significantly improving contrast and science return. This technique is directly applicable to JWST coronagraphs by taking advantage of a new feature recently added to the observatory pointing system, which permits very small dithers using the Fine Steering Mirror with high accuracy under fine-guidance closed loop.

Our simulations suggest that the performance gains over Classical Subtraction are substantial. In particular, SGDs are shown to be mostly insensitive to the actual target acquisition accuracy, yielding consistent improved performance compared to Classical Subtraction. Given the additional exposure time required for the reference images, the use of SGDs will remain optional. Interested observers with challenging science cases will have to weigh the benefits SGDs with the extra exposure time. Finally, SGDs should be beneficial to applications beyond coronagraphy (e.g. slits & micro-shutters calibration) as well as other missions such as WFIRST and HST (with small-angle maneuvers).

ACKNOWLEDGEMENTS

The authors wish to thank the members of the JWST Coronagraphs Working group for interesting discussions. The authors also thank the JWST Line of Sight Working Group for supporting the fine guidance offset maneuver and Northrop Grumman Aerospace Systems for implementing this capability.

REFERENCES

[1] Rieke, M., “The JWST-NIRCam view of the of Galaxy Evolution," in [Galaxy Evolution: Infrared to Millimeter Wavelength Perspective], Wang, W., Lu, J., Luo, Z., Yang, Z., Hua, H., and Chen, Z., eds., PASP 446 , 331 (2011).

[2] Wright, G. S., Rieke, G., Boeker, T., Colina, L., van Dishoeck, E., Driggers, P., Friedman, S., Glasse, A., Goodson, G., Greene, T., Guedel, M., Henning, T., Lagage, P.-O., Lorenzo-Alvarez, J., Meixner, M., Norgaard-Nielsen, H., Olofsson, G., Ray, T., Ressler, M., Sukhatme, K., Thatcher, J., Waelkens, C., and Wright, D., “Progress with the design and development of MIRI, the mid-IR instrument for JWST," in Proc. SPIE 7731 (2010).

[3] Lajoie, C.-P., Soummer, R., Hines, D. C., Rieke, G. H., “Simulations of JWST MIRI 4QPM Coronagraphs Operations and Performances”, Proc. SPIE 9143 (2014).

[4] Soummer, R., Pueyo, L. Larkin, J., “Detection and Characterization of Exoplanets and Disks Using Projections on Karhunen-Loève Eigenimages”, The Astrophysical Journal Letters, 755:L28 (2012).

[5] Lafrenière, D., Marois, C., Doyon, R., Nadeau, D., Artigau, E., “A New Algorithm for Point-Spread Function Subtraction in High-Contrast Imaging: A Demonstration with Angular Differential Imaging”, The Astrophysical Journal, 660, pp770-780 (2007).

[6] Soummer, R., Lajoie, C.-P., Pueyo, L., Hines, D.C., Isaacs, J.C., Nelan, E.P., Clampin, M., Perrin, M., “Small-grid dithering strategy for improved coronagraphic performance with JWST”, Proc. SPIE 9143 (2014)

[7] Perrin, M., Soummer, R., Elliot, E., Lallo, M., Sivaramakrishnan, A., “Simulating point spread functions for the James Webb Space Telescope with WebbPSF”, Proc. SPIE 8842 (2012).

[8] Boccaletti, A. et al., “The Mid-Infrared Instrument for the James Webb Space Telescope, V: Predicted Performance of the MIRI Coronagraphs”, Publications of the Astronomical Society of the Pacific 127:633-645 (2015.

[9] Currie, T. et al., “Deep Thermal Infrared Imaging of HR 8799 bcde: New Atmospheric Constraints and Limits on a Fifth Planet”, The Astrophysical Journal 795:133-148 (2014).